

## On the appearance of caustics for plane sound-wave propagation in moving random media

Ph Blanc-Benon†, D Juvé†, V E Ostashev‡|| and R Wandelt§

† Laboratoire de Mécanique des Fluides et d'Acoustique. URA CNRS 263, Ecole Centrale de Lyon, BP 163 Ecully Cedex, France

‡ Physical Science Laboratory, New Mexico State University, NM 88003-0002, USA

§ Arbeitsgruppe Akustik, Fachbereich Physik, Universität Oldenburg, D-26111 Oldenburg, Germany

Received 10 August 1994

**Abstract.** In this paper we derive expressions for the probability densities for the appearance of the first caustic for a plane sound wave propagating in moving random media. Our approach generalizes the previous work by White *et al* and Klyatskin in the case of motionless media. It allows us to calculate analytically the probability density functions for two- and three-dimensional media and to express these functions in terms of the diffusion coefficient. Explicit equations are given for Gaussian and von Karman spectra of velocity fluctuations. If the random scalar or vectorial fluctuations of the medium have the same contribution to the refractive-index fluctuations, we demonstrate that in a moving medium caustics appear at shorter distances than in a non-moving one. The two-dimensional version of the theory is tested by numerical simulations in the case of velocity fluctuations with Gaussian spectra. Numerical results are in very good agreement with the theoretical predictions.

### 1. Introduction

If a wave propagates in a random medium, at some distance  $x$  from the source caustics appear. The information about this distance, which is conveniently described mathematically by the probability density  $P(x)$  for the distance to the first caustic, is important in many problems. For example, this information gives the range of validity of many tomography methods [1, 2], currently used for remote sensing of the atmosphere and the ocean, because they are valid only in the approximation of geometric optics or acoustics. Furthermore, the distance  $x$  of caustic formation is closely connected [3, 4] to the distance at which the mean-square intensity fluctuation of a wave propagating in a random medium has a maximum. Using the parabolic fourth-moment equation, various authors have performed analytical and numerical calculations for the normalized variance of the intensity fluctuations, i.e. the scintillation index [5–7]. Their results show that the range dependence of the variance of the intensity exhibits a maximum. Moreover, this peaked evolution of the scintillation index is due to the focusing effect of the medium which depends on the characteristic length of the inhomogeneities. Finally, the behaviour of the function  $P(x)$  is of interest for the theory of wave propagation in random media [8–12].

|| On leave from Institute of Atmospheric Physics, Russian Academy of Science, Physzhetskii 3, Moscow 109017, Russia. Present address: Fachbereich Physik, Universität Oldenburg, D-26111 Oldenburg, Germany.

For an initially-plane wave propagating through two-dimensional isotropic turbulence, the probability density  $P_2(x)$  of the distance  $x$  to the first caustic is obtained theoretically in [8] and justified numerically in [9, 10]. The analogous function  $P_3(x)$  for the three-dimensional isotropic turbulence differs from  $P_2(x)$  and is determined theoretically in [11]. For a plane wave propagating through random inhomogeneities delta-correlated in the direction of propagation, the functions  $P_2(x)$  and  $P_3(x)$  are calculated in [12].

In the aforementioned papers [8–12], the probability densities  $P_2(x)$  and  $P_3(x)$  are studied for the case of an initially-plane wave propagating in a motionless random medium. The primary aim of the present paper is to calculate these probability densities for sound-wave propagation in a moving random medium. Such calculations are important for the study of sound propagation in the atmosphere where velocity fluctuations are always noticeable and very often dominate temperature fluctuations, in the upper-mixed oceanic layer and in turbulent currents where current fluctuations may be comparable with sound-speed fluctuations, in the turbulent flows of gases, and so on.

In section 2, the probability densities  $P_2(x)$  and  $P_3(x)$  obtained in [8, 11, 12] are presented. In section 3, the probability density  $P_3(x)$  for a sound wave propagating in a moving random medium with the Gaussian correlation function of random inhomogeneities is calculated. The analogous function  $P_3(x)$  for the von Karman spectrum of random homogeneities is also derived in section 3. In section 4, the probability density  $P_2(x)$  for a sound wave propagating in a two-dimensional moving random medium with the Gaussian correlation function of random inhomogeneities is calculated and compared with a numerical experiment. In the concluding section, section 5, the main results obtained are discussed.

## 2. The probability density for the distance to the first caustic in a motionless medium

Let random inhomogeneities of a motionless medium be located in the half space  $x > 0$  and suppose an initially-plane wave propagates in the direction of the  $x$ -axis incident on this half space from the region  $x < 0$ . We also suppose that random inhomogeneities are statistically homogeneous and delta-correlated in the direction of the  $x$ -axis:

$$\langle \epsilon(x_1 + x, \mathbf{r}_1 + \mathbf{r}) \epsilon(x_1, \mathbf{r}_1) \rangle = B_\epsilon(x, \mathbf{r}) = \delta(x) b_\epsilon(\mathbf{r}) \quad (1)$$

where the function  $\epsilon$  describes fluctuations in the dielectric constant of a medium and is proportional ( $\epsilon = 2n$ ) to refractive index fluctuations  $n$ . In (1)  $\mathbf{r} = (y, z)$  is given in transverse coordinates,  $B_\epsilon$  is the correlation function,  $\delta$  is the delta function, and  $b_\epsilon$  is the transverse correlation function given by:

$$b_\epsilon(\mathbf{r}) = 2\pi \int_{-\infty}^{+\infty} \int_{-\infty}^{+\infty} \Phi_\epsilon(0, \mathbf{K}_\perp) \exp(i\mathbf{K}_\perp \cdot \mathbf{r}) d^2 K_\perp \quad (2)$$

where  $\Phi_\epsilon(K_x, \mathbf{K}_\perp)$  is the three-dimensional spectral density of the random field  $\epsilon$ . We recall the well-known fact [13] that for geometric-acoustic, Rytov and parabolic-equation methods, the Markov approximation (1) is only a suitable and convenient mathematical approximation of the correlation function  $B_\epsilon(x, \mathbf{r})$  which has finite scales  $l_x$  and  $l_r$  in the direction of the  $x$ -axis and the  $yz$ -plane, respectively. We also recall that these scales,  $l_x$  and  $l_r$ , may be different.

Using the Markov approximation (1) and assuming that the random field  $\epsilon$  is isotropic in the  $yz$ -plane, for the problem considered in this section, Klyatskin [12] derived the probability distribution  $P_3(x)$  for the distance  $x$  to the first caustic:

$$P_3(x) = \frac{\alpha}{D_3 x^4} \exp\left(-\frac{\beta}{D_3 x^3}\right) \quad (3)$$

where  $\alpha$  and  $\beta$  are numerical constants, and  $\mathcal{D}_3$  is the diffusion coefficient, given by:

$$\mathcal{D}_3 = \frac{\pi^2}{16} \int_0^\infty K_\perp^5 \Phi_\epsilon(0, K_\perp) dK_\perp. \tag{4}$$

Note that this probability density function and the numerical values of  $\alpha$  and  $\beta$  were first obtained by White [11] using a scaling parameter  $\gamma$  defined in a non-cartesian system of coordinates by

$$\gamma = 2 \int_0^{+\infty} \left( \frac{1}{R} \frac{\partial}{\partial R} \right)^2 B_\epsilon(R) dR$$

with  $R = \sqrt{x^2 + r^2}$ . The diffusion coefficient  $\mathcal{D}_3$  introduced by Klyatskin [12] depends on cartesian coordinates. Taking into account the fact that

$$\Delta_\perp^2 B_\epsilon(x = R, 0, 0) = 8 \left( \frac{1}{R} \frac{\partial}{\partial R} \right)^2 B_\epsilon(R)$$

the coefficients  $\alpha$  and  $\beta$  in (3) must have the values 0.87 and 0.33, respectively, to be in agreement with the results obtained previously by White [11].

Now let us consider our problem for the two-dimensional case when the dependence of all functions on the coordinate  $z$  may be omitted. For two-dimensional turbulence, equations (1) and (2) take the form:

$$\langle \epsilon(x_1 + x, y_1 + y) \epsilon(x_1, y_1) \rangle = B_\epsilon(x, y) = \delta(x) b_\epsilon(y) \tag{5}$$

$$b_\epsilon(y) = 2\pi \int_{-\infty}^{+\infty} \Phi_\epsilon(0, K_y) \exp(iK_y \cdot y) dK_y. \tag{6}$$

These equations also allow us to consider the case when the scales  $l_x$  and  $l_y$  of the correlation function  $B_\epsilon(x, y)$  are different. Using the Markov approximation (5), the probability distribution  $P_2(x)$  is calculated in [8-12]†:

$$P_2(x) = \frac{\nu^2}{\sqrt{2\pi} \mathcal{D}_2 x^{5/2}} \exp\left(-\frac{\nu^4}{6\mathcal{D}_2 x^3}\right) \tag{7}$$

where  $\nu = K(1/2) \simeq 1.85$ ,  $K$  is the complete elliptic integral, and  $\mathcal{D}_2$  is the diffusion coefficient given by:

$$\mathcal{D}_2 = \pi \int_0^\infty K_y^4 \Phi_\epsilon(0, K_y) dK_y. \tag{8}$$

Note that (3) and (7) were first derived in [8] and [11], respectively, for the case of isotropic turbulence where  $l_x = l_r$  and  $l_x = l_y$ . The limit of validity of (3) and (7) is given by the inequality  $\mathcal{D}x^3 \ll 1$  [12].

### 3. Three-dimensional moving random medium

In this section we assume that an initially-plane sound wave incidents on the half space  $x > 0$  where the adiabatic sound speed  $c(\mathbf{R})$  and medium velocity  $\mathbf{v}(\mathbf{R})$  are random functions of the coordinates  $\mathbf{R} = (x, \mathbf{r})$ ,  $\langle c \rangle = c_0$  and  $\langle \mathbf{v} \rangle = 0$ . If  $\mathbf{v} = 0$ , the probability density  $P_3(x)$  of the distance  $x$  to the first caustic for this wave is given by (3) and (4) where  $\Phi_\epsilon$  is the three-dimensional spectral density of the random field:

$$\epsilon = 2n = -2 \frac{\tilde{c}}{c_0}. \tag{9}$$

† In [12] we interpret the additional factor of 3 on the right-hand side of equation (7) as a misprint.

Here  $\tilde{c} = c - c_0$  denotes the sound-speed fluctuations. It is our aim to generalize (3) and (4) to the case  $v \neq 0$ .

### 3.1. Basic equations

This generalization technique is described in [14–16]: in the geometric-acoustic, Rytov and parabolic-equation methods, the statistical characteristics of a sound wave propagating in a moving random medium are given by equations for analogous statistical characteristics for the sound wave propagating in a motionless random medium, where in the latter equations the correlation function  $B_\epsilon(x, r)$  or its three-dimensional spectral density  $\Phi_\epsilon(K_x, \mathbf{K}_\perp)$  is replaced by the effective correlation function  $B_{\text{eff}}(x, r)$  or its spectral density  $\Phi_{\text{eff}}(K_x, \mathbf{K}_\perp)$ , respectively, given by:

$$B_{\text{eff}}(x, r) = B_\epsilon(x, r) + \frac{4}{c_0^2} B_{11}(x, r) \quad (10)$$

$$\Phi_{\text{eff}}(K_x, \mathbf{K}_\perp) = \Phi_\epsilon(K_x, \mathbf{K}_\perp) + \frac{4}{c_0^2} \Phi_{11}(K_x, \mathbf{K}_\perp).$$

Here  $B_{11}$  and  $\Phi_{11}$  are the correlation function and its three-dimensional spectral density for fluctuations of the medium-velocity component  $v_1$  in the direction of the  $x$ -axis; they are connected by the following equation:

$$B_{11}(x, r) = \langle v_1(x_1 + x, r_1 + r) v_1(x_1, r_1) \rangle$$

$$= \int_{-\infty}^{+\infty} dK_x \int_{-\infty}^{+\infty} \int_{-\infty}^{+\infty} d^2 K_\perp \exp(ixK_x + ir \cdot \mathbf{K}_\perp) \Phi_{11}(K_x, \mathbf{K}_\perp). \quad (11)$$

It should be noted here, that even for isotropic turbulence, the functions  $B_{11}(x, r)$ ,  $\Phi_{11}(K_x, \mathbf{K}_\perp)$  and, hence, the functions  $B_{\text{eff}}(x, r)$ ,  $\Phi_\epsilon(K_x, \mathbf{K}_\perp)$  are anisotropic [16]. Therefore, when calculating the probability density  $P_3$  in a statistically isotropic moving random medium we must use (3) and (4) which are valid for an anisotropic motionless random medium. When deriving equation (10), the terms of the order of  $v^2/c^2$  are neglected and it is assumed that  $\nabla \cdot v = 0$  (this assumption is usually valid for turbulent fields). In the Markov approximation, we may put  $K_x = 0$  in (10) (see [15–16]). Moreover, for locally homogeneous and isotropic turbulence (10) takes the form [14–16]:

$$\Phi_{\text{eff}}(0, K_\perp) = \Phi_\epsilon(0, K_\perp) + \frac{4}{c_0^2} F(K_\perp). \quad (12)$$

Here,  $F(K)$  is the three-dimensional spectral density of the isotropic and solenoidal random vector field  $v$ , related [17] to  $\Phi_{11}$  by:

$$\Phi_{11}(K_x, \mathbf{K}_\perp) = \frac{K_\perp^2}{K^2} F(K) \quad (13)$$

where  $K = \sqrt{(K_x^2 + K_\perp^2)}$ . Replacing  $\Phi_\epsilon$  by  $\Phi_{\text{eff}}$  in (3) and (4) yields the probability density for the distance to the first caustic for an initially-plane wave propagating in a moving random medium:

$$P_3(x) = \frac{\alpha}{D_3 x^4} \exp\left(-\frac{\beta}{D_3 x^3}\right) \quad (14)$$

$$D_3 = \frac{\pi^2}{16} \int_0^\infty K_\perp^5 \Phi_{\text{eff}}(0, K_\perp) dK_\perp. \quad (15)$$

Comparing these equations with (3) and (4), we observe that the probability density  $P_3(x)$  is given by the same function for a moving and a motionless medium, but with a different diffusion coefficient  $\mathcal{D}_3$ . Now we calculate this diffusion coefficient for a Gaussian correlation function of random inhomogeneities and for the von Karman spectrum.

### 3.2. Gaussian correlation function

The Gaussian correlation function  $B_\epsilon(\mathbf{R})$  of the statistically homogeneous and isotropic scalar random field  $\epsilon(\mathbf{R})$  and its three-dimensional spectral density  $\Phi_\epsilon(\mathbf{K})$  are widely used in the literature and are given by:

$$B_\epsilon(\mathbf{R}) = \sigma_\epsilon^2 \exp(-R^2/l^2) \quad (16)$$

$$\Phi_\epsilon(\mathbf{K}) = \frac{\sigma_\epsilon^2 l^3}{8\pi^{3/2}} \exp(-K^2 l^2/4). \quad (17)$$

Here  $\sigma_\epsilon^2$  is the variance of the random field  $\epsilon$ ,  $l$  is the scale of inhomogeneities.

As for the medium-velocity component  $v_1(\mathbf{R})$ , we may not prescribe a Gaussian form for its correlation function  $B_{11}$  and its three-dimensional spectral density  $\Phi_{11}(\mathbf{K})$  because, as previously mentioned for the statistically homogeneous and isotropic vector random field  $\mathbf{v}$ , the functions  $B_{11}(\mathbf{R})$  and  $\Phi_{11}(\mathbf{K})$  must be anisotropic. Therefore, following [16], we prescribe the Gaussian correlation function for the longitudinal correlation function of the velocity field  $\mathbf{v}$ :

$$B_{RR}(\mathbf{R}) = \langle v_R(\mathbf{R}_1 + \mathbf{R})v_R(\mathbf{R}_1) \rangle = \sigma_v^2 \exp(-R^2/l^2) \quad (18)$$

where  $v_R$  is the component of the vector  $\mathbf{v}$  in the direction of vector  $\mathbf{R}$ ,  $\sigma_v^2$  is the variance of the random field  $v_R$ . If the random field  $\mathbf{v}$  is additionally solenoidal ( $\nabla \cdot \mathbf{v} = 0$ ), the functions  $B_{11}$  and  $B_{RR}$  are related by:

$$B_{11}(x, r) = B_{RR}(R) + \frac{r^2}{2R} \frac{d}{dR} B_{RR}(R). \quad (19)$$

This equation may be easily obtained from well-known equations (see, for example, [16–18]) for the correlation tensor of a statistically homogeneous and isotropic field  $\mathbf{v}$  and for the relationship between transverse and longitudinal correlation functions of this field. Substituting (18) into (19) yields:

$$B_{11}(x, r) = \sigma_v^2 \left( 1 - \frac{r^2}{l^2} \right) \exp(-R^2/l^2). \quad (20)$$

From this equation we see that  $B_{11}$  is an anisotropic function. Furthermore, from (20), it follows that the variance of the random field  $v_1$  is  $\sigma_v^2$ . Using (11), (13) and (20), we calculate the three-dimensional spectral density  $F(\mathbf{K})$  for the vector random field  $\mathbf{v}$  with the Gaussian longitudinal correlation function:

$$F(\mathbf{K}) = \frac{\sigma_v^2 K^2 l^5}{32\pi^{3/2}} \exp(-K^2 l^2/4). \quad (21)$$

Now we substitute (17) and (21) into (12) and determine the effective spectral density  $\Phi_{\text{eff}}$ . Substituting the function obtained  $\Phi_{\text{eff}}$  into (15) and calculating the integral on the right-hand side of this equation yields the diffusion coefficient  $\mathcal{D}_3$  in a moving random medium:

$$\mathcal{D}_3 = \frac{\sqrt{\pi}}{2l^3} \left( \sigma_\epsilon^2 + 12 \frac{\sigma_v^2}{c_0^2} \right). \quad (22)$$

We denote the variance of sound-speed fluctuations  $\tilde{c}$  by  $\sigma_c^2$ . Then from (9) it follows that  $\sigma_\epsilon^2 = 4\sigma_c^2/c_0^2$ . Using this equation, we may represent (22) in the form:

$$\mathcal{D}_3 = \mathcal{D}_{3,c} + \mathcal{D}_{3,v} = \frac{2\sqrt{\pi}}{l^3 c_0^2} (\sigma_c^2 + 3\sigma_v^2) \tag{23}$$

where

$$\mathcal{D}_{3,c} = \frac{2\sqrt{\pi}}{l^3} \frac{\sigma_c^2}{c_0^2} \quad \text{and} \quad \mathcal{D}_{3,v} = \frac{6\sqrt{\pi}}{l^3} \frac{\sigma_v^2}{c_0^2} \tag{24}$$

are the contributions to the diffusion coefficient  $\mathcal{D}_3$  due to sound-speed and medium-velocity fluctuations, respectively.

It is known (see, for example, [16, 17]) that fluctuations  $n$  in the refractive index of a moving medium in the direction of the  $x$ -axis are given by:

$$n = -\frac{2(\tilde{c} + v_x)}{c_0} \tag{25}$$

It should be noted here that (10) and (12), which are used to derive equations (14) and (15) for  $P_3$  and  $\mathcal{D}_3$ , are obtained on the basis of (23) (see [14–16]). We also note that from (24) it follows that  $\tilde{c}$  and  $v_x$  give the same contribution to  $n$ , and, hence,  $\sigma_c^2$  and  $\sigma_v^2$  give the same contribution to the variance of  $n$ :

$$\sigma_n^2 = \frac{4}{c_0^2} (\sigma_c^2 + \sigma_v^2). \tag{26}$$

On the other hand, from (24) it follows that the contribution to the coefficient  $\mathcal{D}_3$  from  $\sigma_v^2$  is three times greater than that from  $\sigma_c^2$ . This result will be explained below. Replacing  $\mathcal{D}_3$  in (14) first by  $\mathcal{D}_{3,c}$  and then by  $\mathcal{D}_{3,v}$ , we obtain the probability densities  $P_{3,c}(x)$  and  $P_{3,v}(x)$  for the distance  $x$  to the first caustic for a plane sound wave in purely motionless and purely moving random media, respectively.

The functions  $P_{3,c}(x)$  and  $P_{3,v}(x)$  are shown in figure 1 for  $\sigma_c^2/c_0^2 = \sigma_v^2/c_0^2 = 3 \times 10^{-6}$  and  $l = 1.25$  m (according to [19] these values of  $\sigma_c^2/c_0^2$ ,  $\sigma_v^2/c_0^2$  and  $l$  are typical for the atmospheric turbulence near the ground). From figure 1 it follows that  $P_{3,c}(x)$  and  $P_{3,v}(x)$  have maxima at the distances  $x_{3,c}$  and  $x_{3,v}$ , respectively. These distances may be determined from (14):

$$x_{3,c} = \left( \frac{3\beta}{4\mathcal{D}_{3,c}} \right)^{1/3} \quad x_{3,v} = \left( \frac{3\beta}{4\mathcal{D}_{3,v}} \right)^{1/3} \tag{27}$$

These equations are valid for arbitrary values of  $\mathcal{D}_{3,c}$  and  $\mathcal{D}_{3,v}$ . Substituting (24) into (27) yields two distances  $x_{3,c}$  and  $x_{3,v}$  for the given case of Gaussian correlation functions for random inhomogeneities:

$$x_{3,c} = \frac{l}{2} \left( \frac{3\beta c_0^2}{\pi^{1/2} \sigma_c^2} \right)^{1/3} \quad x_{3,v} = \frac{l}{2} \left( \frac{\beta c_0^2}{\pi^{1/2} \sigma_v^2} \right)^{1/3} \tag{28}$$

The distances  $x_{3,c}$  and  $x_{3,v}$  are associated with the space regions where caustics appear most likely, and therefore they are important for the study of sound propagation in random media. From figure 1 and (28) we observe that the distance  $x_{3,v}$  is shorter than the distance  $x_{3,c}$  by a factor  $3^{1/3}$  if  $\sigma_v^2 = \sigma_c^2$ .

The main result obtained in the present paper is that for the same variances of sound-speed and medium-velocity fluctuations ( $\sigma_v^2 = \sigma_c^2$ ), caustics appear in a purely moving random medium at shorter distances than in a purely motionless medium. This is due to the fact that, even for isotropic turbulence, the correlation function  $B_{11}(x, r)$  (see (20))

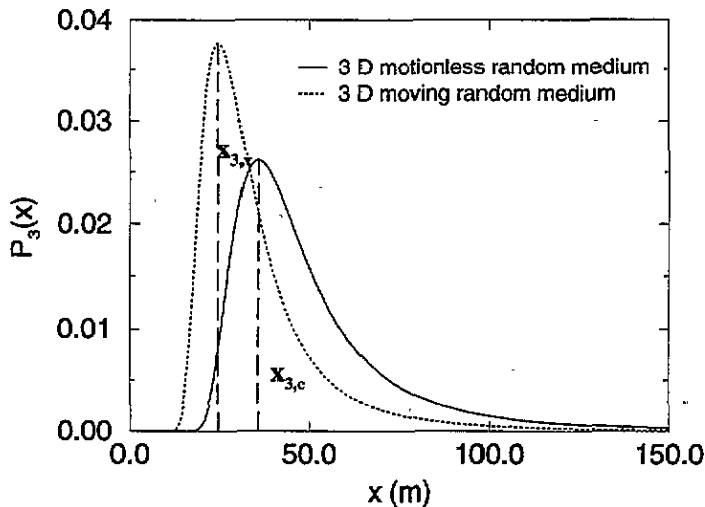


Figure 1. Probability densities for the distance  $x$  to the first caustic for a plane sound wave propagating in three-dimensional random media with Gaussian correlation functions: comparison of a purely moving medium and a purely motionless medium. The functions are represented for  $\sigma_c^2/c_0^2 = \sigma_v^2/c_0^2 = 3 \times 10^{-6}$  and  $l = 1.25$  m. The distances  $x_{3,c}$  and  $x_{3,v}$  associated with the space regions where caustics appear most likely are indicated by dotted vertical lines.

is anisotropic, and therefore moving inhomogeneities disturb the phase front of a sound wave to a greater extent than motionless inhomogeneities which have isotropic correlation function  $B_\epsilon(R)$  (see (16)). It is also well known that the more disturbances there are in a wave front, the shorter the distance of caustic formation is. This also explains why the contribution to  $\mathcal{D}_{3,v}$  from  $\sigma_v^2$  is greater than the contribution from  $\sigma_c^2$ .

Let us denote by  $\Delta x_3 = x_{3,c} - x_{3,v}$  the difference in the distances of most likely caustic formation in purely motionless and moving random media. Using (28), we find:

$$\Delta x_3 = x_{3,c} \left[ 1 - \left( \frac{\sigma_c^2}{3\sigma_v^2} \right)^{1/3} \right]. \tag{29}$$

If  $\sigma_c^2 = \sigma_v^2$ , from this equation it follows that  $\Delta x_3 \approx 0.307x_{3,c}$ .

### 3.3. von Karman spectrum

Now we calculate the values of the diffusion coefficients  $D_{3,c}$  and  $D_{3,v}$  and distances  $x_{3,c}$  and  $x_{3,v}$  for the von Karman spectrum of random inhomogeneities. For this spectrum, the three-dimensional spectral density  $\Phi_\epsilon(K)$  is given by the well-known equation [13]:

$$\Phi_\epsilon(K) = AC_\epsilon^2(K^2 + K_0^2)^{-11/6} \exp(-K^2/K_m^2) \tag{30}$$

where  $A = 5\sqrt{3}\Gamma(2/3)/36\pi^2 \approx 0.033$ ,  $\Gamma$  is the gamma function,  $C_\epsilon^2$  is the structure parameter for fluctuations of the random field  $\epsilon$ ,  $K_0 = 2\pi/L_0$  and  $K_m = 5.92/l_0$ ,  $L_0$  and  $l_0$  are the outer and inner scales of turbulence. The variance  $\sigma_\epsilon^2$  of the random field  $\epsilon$  is given by:

$$\sigma_\epsilon^2 = \int_{-\infty}^{+\infty} \int_{-\infty}^{+\infty} \int_{-\infty}^{+\infty} \Phi_\epsilon(K) d^3K. \tag{31}$$

Substituting into this equation the value of  $\Phi_\epsilon$  given by (30), calculating the integral with respect to  $K$  and assuming that  $K_0 \ll K_m$ , we obtain:

$$\sigma_\epsilon^2 = \frac{6}{5}\pi^{3/2} A \frac{\Gamma(1/3)}{\Gamma(5/6)} C_\epsilon^2 K_0^{-2/3}. \quad (32)$$

Note that the inequality  $K_0 \ll K_m$  is always valid because in turbulent media  $L_0 \gg l_0$ . Equation (32) relates  $\sigma_\epsilon^2$  and  $C_\epsilon^2$  which characterize the intensity of the random field  $\epsilon$ . As for the three-dimensional spectral density  $F(K)$  of the random field  $v$ , its value is given by [20]:

$$F(K) = \frac{11}{6} A C_v^2 K^2 (K^2 + K_0^2)^{-17/6} \exp(-K^2/K_m^2) \quad (33)$$

where  $C_v^2$  is the structure parameter for medium-velocity fluctuations. The variance  $\sigma_v^2$  of the random field  $v_1$  is given by:

$$\sigma_v^2 = \int_{-\infty}^{+\infty} \int_{-\infty}^{+\infty} \int_{-\infty}^{+\infty} \Phi_{11}(K) d^3K = \int_{-\infty}^{+\infty} \int_{-\infty}^{+\infty} \int_{-\infty}^{+\infty} \frac{K_\perp^2}{K^2} F(K) d^3K. \quad (34)$$

When deriving this equation, we use (13). Substituting into (34) the value of  $F$  given by (33) we obtain:

$$\sigma_v^2 = \frac{6}{5}\pi^{3/2} A \frac{\Gamma(1/3)}{\Gamma(5/6)} C_v^2 K_0^{-2/3}. \quad (35)$$

This equation is also valid for  $K_0 \ll K_m$ . Equation (34) relates  $\sigma_v^2$  and  $C_v^2$  which characterize the intensity of the vector random field  $v$ .

Substituting (30) and (34) into (12) yields the effective spectral density for the von Karman spectrum:

$$\Phi_{\text{eff}}(0, K_\perp) = A \left( C_\epsilon^2 + \frac{22}{3} \frac{K_\perp^2}{K_\perp^2 + K_0^2} \frac{C_v^2}{c_0^2} \right) (K_\perp^2 + K_0^2)^{-11/6} \exp(-K_\perp^2/K_m^2). \quad (36)$$

If  $K_0 \rightarrow 0$  and  $K_m \rightarrow \infty$ , (36) becomes an equation for the effective spectral density  $\Phi_{\text{eff}}(0, K_\perp)$  for the Kolmogorov spectrum, which is obtained in [14–16] and is proportional to the effective structure parameter  $C_{\text{eff}}^2$  given by:

$$C_{\text{eff}}^2 = C_\epsilon^2 + \frac{22}{3} \frac{C_v^2}{c_0^2}. \quad (37)$$

Substituting (36) into (15) and calculating the integral on the right-hand side of the latter equation, we find the diffusion coefficient  $\mathcal{D}_3$  in a medium with the von Karman spectrum of random inhomogeneities:

$$\mathcal{D}_3 = \frac{\pi^2}{16} A K_0^{7/3} \left[ C_{\text{eff}}^2 \Psi \left( 3, \frac{13}{6}; \frac{K_0^2}{K_m^2} \right) + \frac{22}{3} \frac{C_v^2}{c_0^2} \Psi \left( 4, \frac{13}{6}; \frac{K_0^2}{K_m^2} \right) \right] \quad (38)$$

where  $\Psi$  is the confluent hypergeometric function. Replacing in (38) the functions  $\Psi$  by their asymptotics for  $K_0^2/K_m^2 \rightarrow 0$ , we obtain:

$$\mathcal{D}_3 = \frac{\pi^2}{32 \times 4} A \Gamma(1/6) K_m^{7/3} \left( C_\epsilon^2 + \frac{22}{3} \frac{C_v^2}{c_0^2} \right). \quad (39)$$

Note that from (37) and (39) it follows that  $\mathcal{D}_3$  is proportional to  $C_{\text{eff}}^2$ . Substituting the values of  $C_\epsilon^2$  and  $C_v^2$  given by (32) and (35), respectively, into (39) and using the equality  $C_\epsilon^2 = 4C_v^2/c_0^2$ , we obtain:

$$\mathcal{D}_3 = \mathcal{D}_{3,c} + \mathcal{D}_{3,v} = \frac{5\pi^{3/2}}{2^4 3^2 \Gamma(1/3)} \frac{K_m^{7/3} K_0^{2/3}}{c_0^2} \left( \sigma_c^2 + \frac{11}{6} \sigma_v^2 \right) \quad (40)$$

where

$$D_{3,c} = \frac{5\pi^{3/2}}{2^4 3^2 \Gamma(1/3)} K_m^{7/3} K_0^{2/3} \frac{\sigma_c^2}{c_0^2} \quad \text{and} \quad D_{3,v} = \frac{55\pi^{3/2}}{2^5 3^3 \Gamma(1/3)} K_m^{7/3} K_0^{2/3} \frac{\sigma_v^2}{c_0^2} \quad (41)$$

are the contributions to the diffusion coefficient  $D_3$  due to sound-speed and medium-velocity fluctuations, respectively. From (40) it follows that the contribution to the diffusion coefficient  $D_3$  from the medium-velocity fluctuations exceeds that from the sound-speed fluctuations by a factor 11/6. We recall that for the Gaussian correlation function this factor is 3, see (24).

For the von Karman spectrum, the probability densities  $P_{3,c}(x)$  and  $P_{3,v}(x)$  have an analogous form to the probability densities for the Gaussian correlation function considered above, see figure 1. The distances  $x_{3,c}$  and  $x_{3,v}$  at which  $P_{3,c}(x)$  and  $P_{3,v}(x)$  are maximal may be found if we substitute (41) into (27):

$$x_{3,c} = \left( \frac{2^2 3^3 \Gamma(1/3) \beta c_0^2}{5\pi^{3/2} K_m^{7/3} K_0^{2/3} \sigma_c^2} \right)^{1/3} \quad x_{3,v} = \left( \frac{2^3 3^4 \Gamma(1/3) \beta c_0^2}{55\pi^{3/2} K_m^{7/3} K_0^{2/3} \sigma_v^2} \right)^{1/3} \quad (42)$$

From these equations it follows that the distance  $\Delta x_3 = x_{3,c} - x_{3,v}$  between the maxima of the probability densities  $P_{3,c}(x)$  and  $P_{3,v}(x)$  is given by:

$$\Delta x_3 = x_{3,c} \left[ 1 - \left( \frac{6\sigma_c^2}{11\sigma_v^2} \right)^{1/3} \right] \quad (43)$$

If  $\sigma_c^2 = \sigma_v^2$ , from (43) it follows that  $\Delta x_3 \simeq 0.183x_{3,c}$ .

#### 4. Two-dimensional moving random medium

In this section we calculate analytically the probability density  $P_2(x)$  for the distance  $x$  to the first caustic for an initially-plane sound wave incidenting on the two-dimensional half space  $x > 0$  with random inhomogeneities of  $\tilde{c}$  and  $v$ . These calculations are of interest because we are able to compare them with analogous results obtained by numerical simulation [10].

##### 4.1. Basic equations

Let us introduce the effective spectral density:

$$\Phi_{\text{eff}}(K_x, K_y) = \Phi_\epsilon(K_x, K_y) + \frac{4}{c_0^2} \Phi_{11}(K_x, K_y). \quad (44)$$

By analogy with [14–16], it may be shown that statistical characteristics of a sound wave propagating in a two-dimensional moving random medium are the same as the corresponding characteristics in a motionless medium with  $\Phi_\epsilon$  in the latter replaced by  $\Phi_{\text{eff}}$ .

The two-dimensional spectral densities  $\Phi_\epsilon(K)$  and  $\Phi_{11}(K)$  are related to the correlation functions  $B_\epsilon(r)$  and  $B_{11}(r)$  by:

$$B_\epsilon(r) = \int_{-\infty}^{+\infty} \int_{-\infty}^{+\infty} \Phi_\epsilon(K) \exp(iK \cdot r) d^2K \quad (45)$$

$$B_{11}(r) = \int_{-\infty}^{+\infty} \int_{-\infty}^{+\infty} \Phi_{11}(K) \exp(iK \cdot r) d^2K \quad (46)$$

where  $K = (K_x, K_y)$  and  $r = (x, y)$ . The function  $B_{11}$  may also be expressed in terms of the longitudinal  $B_{rr}$  and transverse  $B_{tt}$  correlation functions of the statistically homogeneous and isotropic vector random field  $v = (v_x, v_y)$  (see, for example, [18]):

$$B_{11}(r) = \frac{x^2}{r^2} B_{rr}(r) + \frac{y^2}{r^2} B_{tt}(r). \quad (47)$$

If the field  $v$  is additionally solenoidal, the functions  $B_{tt}$  and  $B_{rr}$  are connected by:

$$B_{tt}(r) = B_{rr}(r) + r \frac{d}{dr} B_{rr}(r). \quad (48)$$

In the Markov approximation, (40) becomes:

$$\Phi_{\text{eff}}(0, K_y) = \Phi_\epsilon(0, K_y) + \frac{4}{c_0^2} \Phi_{11}(0, K_y). \quad (49)$$

#### 4.2. Gaussian correlation function

As in the three-dimensional case, we prescribe Gaussian correlation functions for the functions  $B_\epsilon(r)$  and  $B_{rr}(r)$ :

$$B_\epsilon(r) = \sigma_\epsilon^2 \exp(-r^2/l^2) \quad (50)$$

$$B_{rr}(r) = \sigma_v^2 \exp(-r^2/l^2). \quad (51)$$

Using (45) and (50), we calculate the two-dimensional spectral density  $\Phi_\epsilon(0, K_y)$  of the random field  $\epsilon$ :

$$\Phi_\epsilon(0, K_y) = \frac{\sigma_\epsilon^2 l^2}{4\pi} \exp(-K_y^2 l^2/4). \quad (52)$$

Making use of (46)–(48) and (51), it is straightforward to calculate the two-dimensional spectral density  $\Phi_{11}(0, K_y)$  of the random field  $v_x$ :

$$\Phi_{11}(0, K_y) = \frac{\sigma_v^2 l^4 K_y^2}{8\pi} \exp(-K_y^2 l^2/4). \quad (53)$$

Substituting (48) and (49) into (45), we obtain the effective spectral density for the Gaussian correlation functions of random inhomogeneities:

$$\Phi_{\text{eff}}(0, K_y) = \frac{l^2}{4\pi} \left( \sigma_\epsilon^2 + \frac{\sigma_v^2 l^2 K_y^2}{2} \right) \exp(-K_y^2 l^2/4). \quad (54)$$

Substituting this equation into the right-hand side of (18), calculating the integral with respect to  $K_y$  and using (7), we find the probability density for the distance to the first caustic for an initially-plane wave propagating in a two-dimensional moving medium:

$$P_2(x) = \frac{v^2}{\sqrt{2\pi D_2} x^{5/2}} \exp(-v^4/6D_2 x^3) \quad (55)$$

where the diffusion coefficient  $D_2$  is given by:

$$D_2 = \frac{3\sqrt{\pi}}{l^3} \left( \sigma_\epsilon^2 + 20 \frac{\sigma_v^2}{c_0^2} \right). \quad (56)$$

As in the three-dimensional case, in (56) we replace  $\sigma_\epsilon^2$  by  $4\sigma_c^2/c_0^2$  and represent this equation in the form:

$$D_2 = D_{2,c} + D_{2,v} = \frac{12\sqrt{\pi}}{l^3 c_0^2} (\sigma_c^2 + 5\sigma_v^2) \quad (57)$$

where

$$\mathcal{D}_{2,c} = \frac{12\sqrt{\pi}}{l^3} \frac{\sigma_c^2}{c_0^2} \quad \text{and} \quad \mathcal{D}_{2,v} = \frac{60\sqrt{\pi}}{l^3} \frac{\sigma_v^2}{c_0^2} \quad (58)$$

are the contributions to the diffusion coefficient  $\mathcal{D}_2$  due to the sound-speed and medium-velocity fluctuations, respectively. From (57) it follows that the contribution to  $\mathcal{D}_2$  from  $\sigma_v^2$  exceeds that from  $\sigma_c^2$  by a factor 5. Note that in the three-dimensional case the value of this factor is 3, see (24).

Replacing  $\mathcal{D}_2$  in (55) by  $\mathcal{D}_{2,c}$  and  $\mathcal{D}_{2,v}$  we find the probability densities  $P_{2,c}(x)$  and  $P_{2,v}(x)$  for the distance  $x$  to the first caustic for a plane sound wave propagating in a purely motionless and a purely moving random media, respectively. These probability densities are shown in figure 2 for the same values of  $\sigma_c^2/c_0^2$ ,  $\sigma_v^2/c_0^2$  and  $l$  as in figure 1 (i.e.  $\sigma_c^2/c_0^2 = \sigma_v^2/c_0^2 = 3 \times 10^{-6}$  and  $l = 1.25$  m).

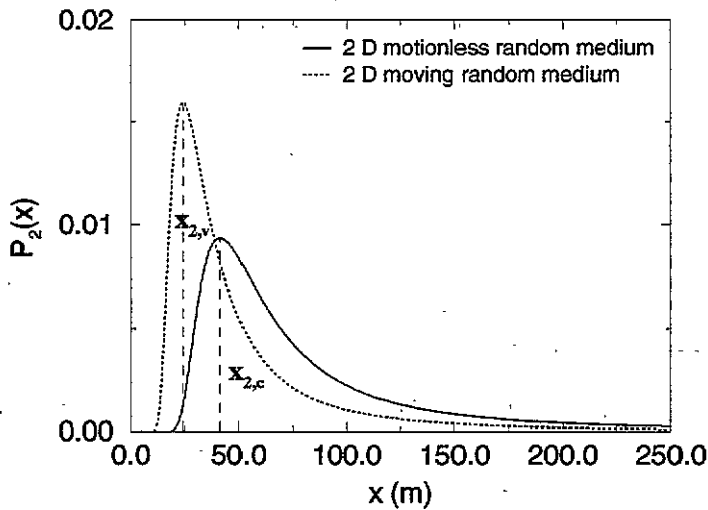


Figure 2. Probability densities for the distance  $x$  to the first caustic for a plane sound wave propagating in two-dimensional random media with Gaussian correlation functions: comparison of a purely moving medium and a purely motionless medium. The functions are represented for  $\sigma_c^2/c_0^2 = \sigma_v^2/c_0^2 = 3 \times 10^{-6}$  and  $l = 1.25$  m. The distances  $x_{2,c}$  and  $x_{2,v}$  associated with the space regions where caustics appear most likely are indicated by dotted vertical lines.

Using (55) and (58), we obtain that  $P_{2,c}(x)$  and  $P_{2,v}(x)$  are maximal at the distances:

$$x_{2,c} = l \left( \frac{v^4 c_0^2}{60\pi^{1/2} \sigma_c^2} \right)^{1/3} \quad \text{and} \quad x_{2,v} = l \left( \frac{v^4 c_0^2}{300\pi^{1/2} \sigma_v^2} \right)^{1/3} \quad (59)$$

respectively. The difference  $\Delta x_2 = x_{2,c} - x_{2,v}$  between these distances is given by:

$$\Delta x_2 = x_{2,c} \left[ 1 - \left( \frac{\sigma_c^2}{5\sigma_v^2} \right)^{1/3} \right]. \quad (60)$$

If  $\sigma_v^2 = \sigma_c^2$ , from (60) it follows that  $\Delta x_2 = 0.415x_{2,c}$ .

### 4.3. Comparison with numerical simulations

In [20], Blanc-Benon *et al* introduced a numerical technique to investigate the characteristics of acoustic-ray propagation through simulated turbulent velocity fields. The technique

involves two elements: the generation of a random isotropic vectorial field by means of a superposition of a finite number of discrete Fourier modes; and the integration of the ray-trace equations of geometric acoustics to describe the trajectories of rays and the evolution of the ray-tube area. Assuming that the turbulent field is frozen during the transit time of the acoustic wave, the medium can be modelled, as usual, by a sequence of independent realizations of a random field. The velocity  $v$  at a given point  $r$  is simulated as a sum of  $N$  random incompressible Fourier modes:

$$v(r) = \sum_{l=1}^N U(K^l) \cos(K^l \cdot r + \psi^l) \quad (61)$$

$$U(K^l) \cdot K^l = 0. \quad (62)$$

The direction of the wavevector  $K^l$  and the phase  $\psi^l$  are independent random variables with uniform distributions. For a wavevector  $K^l$ , the amplitude  $\|U(K^l)\|$  associated with that mode is set according to a given two-dimensional kinetic-energy spectrum  $E(K)$ :

$$\|U(K^l)\| = \sqrt{E(K)\Delta K} \quad (63)$$

where  $\Delta K$  is the distance in wavenumber to the next Fourier mode and  $K$  is the length of the wavevector  $K^l$ . For a Gaussian correlation function  $B_{rr}(r)$  (see (51)), we obtain:

$$E(K) = \frac{\sigma_v^2}{8} K^3 l^4 \exp(-K^2 l^2/4). \quad (64)$$

In our simulations, this spectrum has been sampled with  $N = 50$  modes linearly distributed between  $K_{\min} = 0.1/l$  and  $K_{\max} = 10/l$ .

The geometric-acoustic approximation gives a clear visualization of the focusing or defocusing properties of an inhomogeneous medium. It is well suited for computing the ray trajectories and the exact position of caustics along the ray path. In this high-frequency approximation, the acoustic pressure is written in the form:

$$p(x, t) = A(x) \exp[iS(x)] \exp(-i\omega t). \quad (65)$$

The amplitude  $A(x)$  and the local wavevector  $k(x) = \nabla(S)$  are assumed to vary slowly on the scale of a wavelength  $\lambda = 2\pi c_0/\omega$ . An asymptotic expansion for  $\omega \rightarrow \infty$  of the exact linearized equations from fluid mechanics gives the dispersion relation for acoustic waves propagating in an inhomogeneous medium in steady motion [21]:

$$\omega = kc + k \cdot v \quad (66)$$

where  $k$  is the modulus of the acoustic wavenumber  $k$  and  $c$  is the local speed of sound in the medium; in our case we have  $c = c_0$

The rays are the lines tangent to the group velocity  $c_g$  ( $c_g = c_0\nu + v$ ;  $\nu = k/k$ ). They can be determined as the characteristic lines of the dispersion relation through the following Hamiltonian system [22]:

$$\begin{aligned} \frac{dx_i}{dt} &= c_0 \frac{p_i}{1 - p_j M_j} + v_i & \frac{dp_i}{dt} &= -p_j \frac{\partial v_j}{\partial x_i} \\ p &= \frac{1}{1 + M \cdot \nu} \end{aligned} \quad (67)$$

where  $p$  is a dimensionless wavevector ( $p = p\nu$ ) and  $M$  is the Mach number  $v/c_0$ . The rays have been parameterized by the transit time  $t$  from the source to a given point. The position vector  $x = (x, y)$  and the wavevector  $p$  at a current point on the ray trajectory are

completely determined by the value of  $t$  and the initial position along the incident wave front. For an incident plane wave the initial conditions are:

$$\mathbf{x}(t=0) = \begin{pmatrix} 0 \\ y^0 \end{pmatrix} \quad \mathbf{p}(t=0) = \frac{1}{1+M \cdot \nu} \begin{pmatrix} 1 \\ 0 \end{pmatrix}. \quad (68)$$

Plotting the rays permits a clear visualization of the trajectories followed by the acoustic energy radiating from a source. The spatial distribution of rays is a qualitative indicator of the local intensity of the field, since the square root of the amplitude is inversely proportional to the cross-sectional area of a ray tube. In order to determine more precisely the caustics, which are defined as the envelopes of families of rays where the ray-tube section vanishes, we need additional differential equations. In two dimensions, for a plane wave, the two geodesic elements  $\mathbf{R} = (\partial \mathbf{x} / \partial y^0)_i$  and  $\mathbf{Q} = (\partial \mathbf{p} / \partial y^0)_i$ , govern the evolution of the wave front along each ray and permit the evaluation of the cross-sectional area of an infinitesimal ray tube:

$$\frac{dR_i}{dt} = \frac{c_0}{p} (Q_i - v_i v_j Q_j) + c_0 R_j \frac{\partial M_i}{\partial x_j} \quad \frac{dQ_i}{dt} = -c_0 Q_j \frac{\partial M_j}{\partial x_i}. \quad (69)$$

These differential equations require appropriate initial conditions. If we expand  $\mathbf{x}(t, y^0)$  and  $\mathbf{p}(t, y^0)$  using a Taylor series near the origin ( $t \rightarrow 0$ ) for an initially-plane wave, we obtain:

$$\mathbf{R}(t=0) = \begin{pmatrix} 0 \\ 1 \end{pmatrix} \quad \mathbf{Q}(t=0) = \frac{\partial \mathbf{p}(0)}{\partial y^0} \begin{pmatrix} 1 \\ 0 \end{pmatrix}. \quad (70)$$

We solved the system of differential equations (67)–(69) by a Runge–Kutta fourth-order scheme. The time step is  $dt = 1/c_0 K_{\max}$ . It is important to note that the description of the velocity  $\mathbf{v}(\mathbf{r})$  in terms of Fourier modes, allows us to obtain all the spatial derivatives needed to resolve the differential system analytically. Numerical errors are then reduced and computation time is saved in comparison with the usual finite-difference approximations (see also [20, 23] for further discussions on the numerical scheme).

To evaluate the probability of occurrence of the first caustic we launch a family of 81 rays equally spaced in the transversal direction  $y$  between  $y_{\min} = -15l$  and  $y_{\max} = +15l$ . For each ray, the integration of the ray-trace equations is stopped when the ray reaches the position of the caustics. Using an ensemble of 200 realizations, we evaluate the probability distribution over 16200 samples with 256 classes. In these simulations we have used three velocity fields with the same scale  $l$  ( $l = 0.1$  m) and three different values of  $\sigma_v$  ( $1 \text{ m s}^{-1}$ ;  $2 \text{ m s}^{-1}$ ;  $4 \text{ m s}^{-1}$ ). In figures 3–5 we compare the probability density function obtained in our numerical simulation with the theoretical prediction deduced from (55) with  $\mathcal{D}_2 = \mathcal{D}_{2,v}$ . For each of these probability distributions we have similar trends. For short distances of propagation there are no caustics, then we observe a sharp peak at a fixed distance which corresponds exactly to the theoretical value  $x_{2,v}$  deduced from (59). As noted by Klyatskin [12], the condition for application of (7) is in principle  $\mathcal{D}_2 x^3 \ll 1$ . However, with our numerical modelling we demonstrate that expression (7) is valid up to the position of the maximum of the distribution  $x_{2,v}$  for which  $\mathcal{D}_2 x^3 = 1$ . For larger distances, where our theoretical prediction is no longer valid, we observe an exponential decay of the probability density function with the distance of propagation. In [10] we have shown that this decay is in agreement with the results of Kulkarny and White (see [10] for comparison).

Finally, the probability distributions obtained from our numerical simulations have been normalized and plotted in terms of the dimensionless distance  $\tau = \mathcal{D}_{2,v}^{1/3} x$ . Using this

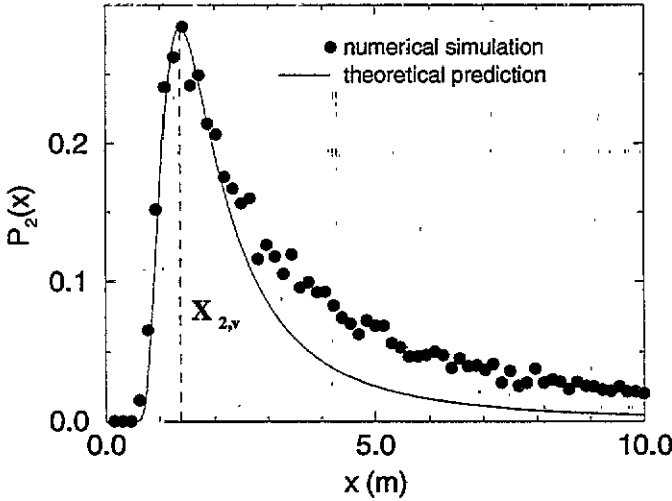


Figure 3. Probability densities for the distance  $x$  to the first caustic for a plane sound wave propagating in two-dimensional Gaussian random moving media: comparison of theory and numerical simulation. The functions are represented for  $\sigma_v = 1 \text{ m s}^{-1}$  and  $l = 0.1 \text{ m}$ . The theoretical distance  $x_{2,v}$  associated with the space regions where caustics appear most likely is indicated by a dotted vertical line.

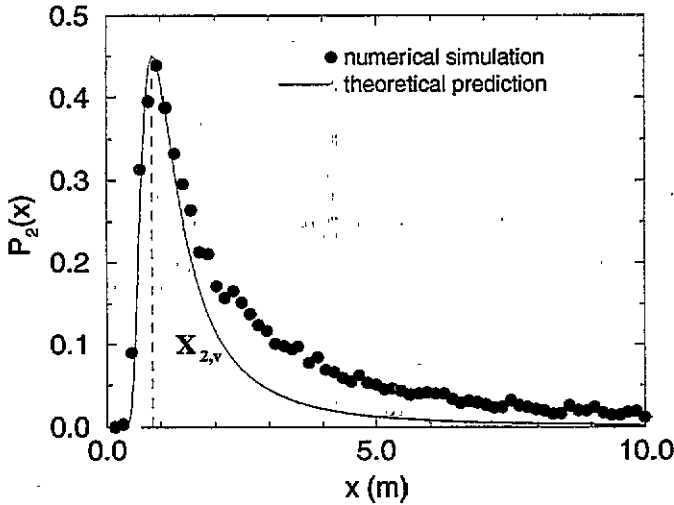


Figure 4. Probability densities for the distance  $x$  to the first caustic for a plane sound wave propagating in two-dimensional Gaussian random moving media: comparison of theory and numerical simulation. The functions are represented for  $\sigma_v = 2 \text{ m s}^{-1}$  and  $l = 0.1 \text{ m}$ . The theoretical distance  $x_{2,v}$  associated with the space regions where caustics appear most likely is indicated by a dotted vertical line.

scaled distance the probability density  $P_2(\tau)$  is now given by:

$$P_2(\tau) = \frac{v^2}{\sqrt{2\pi} \tau^{5/2}} \exp(-v^4/6\tau^3). \quad (71)$$

In figure 6 we note that all the data are in a very good agreement with the theoretical prediction for  $\tau \leq 2$ . In addition, the peak of the probability density function appears at a

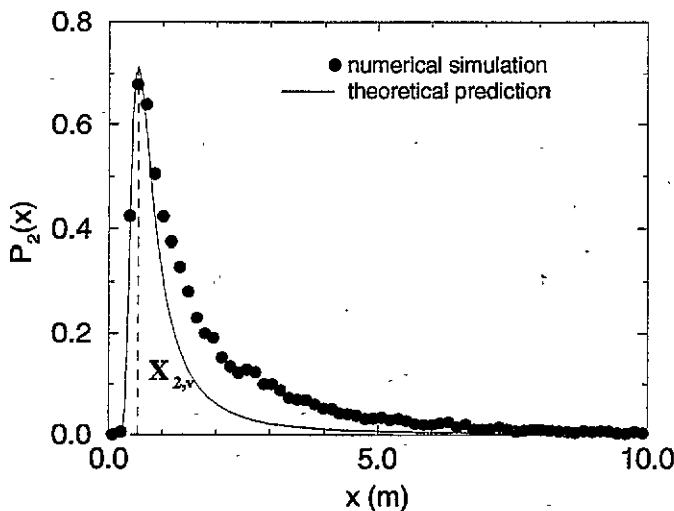


Figure 5. Probability densities for the distance  $x$  to the first caustic for a plane sound wave propagating in two-dimensional Gaussian random moving media: comparison of theory and numerical simulation. The functions are represented for  $\sigma_v = 4 \text{ m s}^{-1}$  and  $l = 0.1 \text{ m}$ . The theoretical distance  $x_{2,v}$  associated with the space regions where caustics appear most likely is indicated by a dotted vertical line.

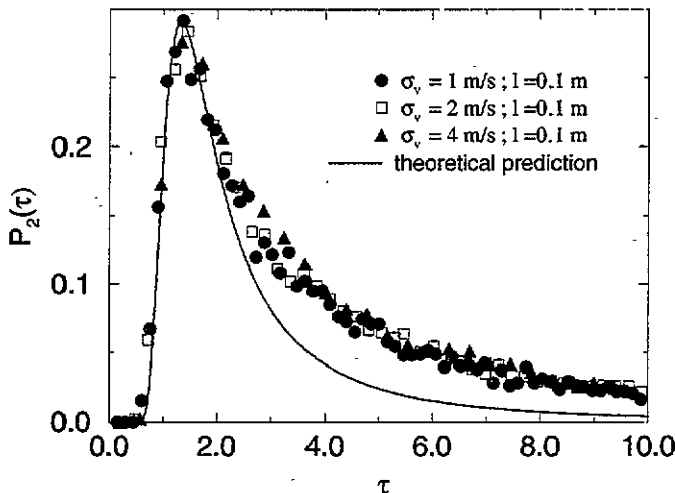


Figure 6. Normalized probability densities for the occurrence of the first caustic for a plane sound wave propagating in two-dimensional Gaussian random moving media: comparison of theory and numerical simulation. The distances are represented in terms of the dimensionless distance  $\tau = \mathcal{D}_{2,v}^{1/3} x$ .

normalized distance  $\tau$  equal to  $(v^4/5)^{1/3} \simeq 1.33$ . From this curve we can obtain an estimate of the distance at which the formation of the first caustic is most probable. We also observe that all the data of our numerical simulation are very well grouped together in terms of the dimensionless distance  $\tau$ .

## 5. Conclusion

In this paper we calculate the probability density functions for the occurrence of the first caustic for a plane wave propagating in a moving random medium. We demonstrate that these probability density functions are given by the functions already calculated for the case of plane wave propagating in a motionless random medium, with different expressions for the diffusion coefficient. The diffusion coefficient has been calculated for two- and three-dimensional random media with the Gaussian and von Karman spectra of random inhomogeneities. One important result is that for the same variance of sound-speed and medium-velocity fluctuations, caustics appear at shorter distances in a purely moving random medium than in a purely motionless one. Finally, a numerical experiment has been performed in the case of a two-dimensional moving medium with the Gaussian correlation function of medium velocity. The results obtained are in very good agreement with the theoretical analysis. Our numerical modelling indicates that the theoretical expression derived for the probability density function is valid up to the distance of propagation corresponding to the maximum of this probability distribution. As a consequence, this distance, which is important in practical applications, is very well predicted by our theory.

## Acknowledgments

This work was carried out while V E Ostashev was a visiting professor at the Ecole Centrale de Lyon, with financial support from the French Ministry of Education. In addition, the authors would thank Professor G Comte-Bellot for her constructive comments.

## References

- [1] Spiesberger J L 1985 Ocean acoustic tomography: travel time biases *J. Acous. Soc. Am.* **77** 83-100
- [2] Wilson D K and Thomson D W Acoustic tomographic monitoring of the atmospheric surface layer *Proc. 5th Int. Symp. on Long-Range Sound Propagation* (Milton Keynes: Faculty of Technology, Open University) pp 249-62
- [3] Juvé D, Blanc-Benon Ph and Comte-Bellot G 1991 Transmission of acoustic waves through mixing layers and 2D isotropic turbulence *Turbulence and Coherent Structures* (Dordrecht: Kluwer) pp 367-84
- [4] Frankenthal S, Whitman A M and Beran M J 1984 Two-scale solutions for intensity fluctuations in strong scattering *J. Opt. Soc. Am. A* **1** 585-97
- [5] Tur M 1982 Numerical solutions for the fourth moment of a plane wave propagating in a random medium *J. Opt. Soc. Am.* **72** 1683-91
- [6] Uscinski B J 1985 Analytical solution of the fourth moment equation and interpretation as a set of phase screens *J. Opt. Soc. Am.* **2** 2077-91
- [7] Blanc-Benon Ph, Juvé D and Hugon-Jeannin Y 1992 Propagation of acoustic waves through thermal turbulence: a numerical study of intensity fluctuations *Proc. European Conf. on Underwater Acoustics* (London: Elsevier) 284-7
- [8] Kulkarny V A and White B S 1982 Focusing of waves in turbulent inhomogeneous media *Phys. Fluids* **25** 1770-84
- [9] Hesselink L and Sturtevant B 1988 Propagation of weak shocks through a random medium *J. Fluid Mech.* **196** 513-53
- [10] Blanc-Benon Ph, Juvé D and Comte-Bellot G 1991 Occurrence of caustics for high-frequency acoustic waves propagating through turbulent fields *Theoret. and Comput. Fluid Dynamics* **2** 271-8
- [11] White B S 1984 The stochastic caustic *J. Appl. Math.* **44** 127-49
- [12] Klyatskin V I 1993 Caustics in random media *Waves Random Media* **3** 93-100
- [13] Rytov S M, Kravtsov Yu A and Tatarskii V I 1989 *Principles of Statistical Radio Physics. Part 4. Wave Propagation Through Random Media* (Berlin: Springer)
- [14] Ostashev V E 1991 Propagation and scattering of sound waves in turbulent media (the atmosphere and ocean) *Atmospheric Optics* **4** 931-7 Engl. transl.

- [15] Ostashev V E 1992 *Sound Propagation in Moving Media* (Moscow: Nauka)
- [16] Ostashev V E 1994 Sound propagation and scattering in media with random inhomogeneities of sound speed, density and medium velocity *Waves Random Media* **4** 403–28
- [17] Tatarskii V I 1971 *The Effects of the Turbulent Atmosphere on Wave Propagation* (Jerusalem: IPST Keter Press)
- [18] Comte-Bellot G 1985 *Turbulence* Ecole Centrale de Lyon
- [19] Daigle G A, Piercy J E and Embleton T F W 1983 Line-of-sight propagation through atmospheric turbulence near the ground *J. Acous. Soc. Am.* **74** 1505–13
- [20] Blanc-Benon Ph, Juvé D, Karweit M and Comte-Bellot G 1990 Simulation numérique de la propagation des ondes acoustiques à travers une turbulence cinématique *J. d'Acoustique* **3** 1–8
- [21] Candel S M 1977 Numerical solution of conservation equations arising in linear wave theory: applications to aeroacoustics *J. Fluid Mech.* **83** 465–93
- [22] Whitham G B 1974 *Linear and Nonlinear Waves* (New York: Wiley)
- [23] Karweit M, Blanc-Benon Ph, Juvé D and Comte-Bellot G 1991 Simulation of the propagation of an acoustic wave through a turbulent velocity field: a study of phase variance *J. Acous. Soc. Am.* **89** 52–62